Journal of Power Sources 251 (2014) 459–465

Contents lists available at ScienceDirect

Journal of Power Sources

journal homepage: www.elsevier.com/locate/jpowsour

Exploration of hydrogen generation from an Mg–$LiBH_4$ system improved by $NiCl_2$ addition

Yongan Liu [a], Xinhua Wang [a,*], Haizhen Liu [a], Zhaohui Dong [a], Guozhou Cao [a], Mi Yan [b]

[a] Key Laboratory of Advanced Materials and Applications for Batteries of Zhejiang Province and Department of Materials Science and Engineering, Zhejiang University, Hangzhou 31007, China
[b] State Key Laboratory of Silicon Materials, Zhejiang University, Hangzhou 310027, China

HIGHLIGHTS

- Novel effects of $LiBH_4$ and $NiCl_2$ on hydrolysis of Mg have been studied.
- A synergistic effect between Mg and $LiBH_4$ has been found primarily.
- Milling time and sample composition are vital factors affecting the hydrolysis.
- Effects of *in situ* deposition of Ni on the hydrolysis have been investigated.

ARTICLE INFO

Article history:
Received 20 September 2013
Received in revised form
7 November 2013
Accepted 26 November 2013
Available online 7 December 2013

Keywords:
Hydrogen generation
Magnesium
Ball milling
Lithium borohydride
Nickel chloride
Hydrolysis

ABSTRACT

A novel method to promote the Mg–H_2O hydrolysis reaction is proposed. Among the hydrides tested, $LiBH_4$ offers the best performance. By ball-milling Mg powder with $LiBH_4$, the maximum hydrogen generation rate (mHGR) and yield are significantly increased. More importantly, the hydrolysis properties are further improved when $NiCl_2$ is added. The newly formed Mg–$LiBH_4$–$NiCl_2$ system reaches an mHGR of 1655 ml min^{-1} g^{-1} and yield of 96.1%. The factors influencing the hydrogen generation performance of this system, such as sample composition and milling time, are investigated. Different methods of characterization, such as X-ray diffraction, X-ray photoelectron spectroscopy and scanning electron microscopy are used for the preliminary mechanistic study. The milling conditions and the *in situ* deposition of metallic Ni are both believed to be important factors that benefit the overall hydrolysis process.

1. Introduction

The technology to develop hydrogen-based fuel cells has become more and more important as burning traditional fossil fuels has brought about severe environmental pollution and energy crisis [1–4]. And first of all a proper hydrogen source is required. Traditional methods which produce hydrogen from fossil fuel, natural gas, and methanol are not suitable because of the CO_2 emissions [5]. Since the late-1990s [6] on-board hydrogen production via the hydrolysis of $NaBH_4$ has attracted much attention because this method has many advantages: high capacity (10.8 wt.%), satisfactory reaction controllability, mild operation conditions, *etc* [7,8]. Nonetheless, $NaBH_4$ has recently been banned for on-board hydrogen storage [9] for its high cost, limited solubility, and necessity of expensive catalysts.

Instead of hydrides, the hydrolysis of light weight metal Mg and Mg based materials is found to be a new way to produce large volume of hydrogen at low cost. The theoretical hydrogen yield of Mg is 8.2 wt. % (no water included in the calculation). The problem is that the reaction is blocked by the $Mg(OH)_2$ byproduct which hinders its use as a hydrogen source. Up to now much work has been done to overcome this problem. Uan et al. [10] catalyzed the hydrolysis of Mg alloy scraps by grinding the Pt-coated Ti net onto the surface of Mg samples and the H_2 generation rate was significantly improved to 432.4 ml min^{-1} (g of catalyst)$^{-1}$ over 8100 s. In a more economical way, they also found that large volume of H_2 could be generated by simply dipping low-grade Mg scrap in seawater to which citric acid had been added [11]. Grosjean et al. [12] improved the hydrogen yield by ball-milling and the 0.5 h

* Corresponding author. Tel./fax: +86 571 8795 2716.
E-mail addresses: xinhwang@zju.edu.cn (X. Wang), mse_yanmi@zju.edu.cn (M. Yan).

0378-7753/$ – see front matter © 2013 Elsevier B.V. All rights reserved.
http://dx.doi.org/10.1016/j.jpowsour.2013.11.104

milled Mg-10 at% Ni composite reached 100% yield in 1 M KCl solution. They believed that the numerous micro galvanic cells formed during ball-milling contributed to the accentuation of the hydrolysis. Besides, ball milling Mg with different salts was also found to be an effective way to optimize the hydrolysis properties of Mg powder [13]. But the effects of ball milling with other hydrides, such as $LiBH_4$, have not been clarified up to now. Hydrides are known to have high gravimetric and volumetric hydrogen capacity [14,15], and $LiBH_4$ is claimed to obtain the largest hydrogen content among them [16]. Kojima et al. [17] studied the hydrolysis properties of $LiBH_4$ and found that the hydrolysis kinetics and yield could be improved by using a stoichiometric amount of water. And Weng et al. [18] realized 100% hydrolysis of $LiBH_4$ by doping it with multiwalled carbon nanotubes. However, as is the case with $NaBH_4$, $LiBH_4$ is also very expensive and its hydrolysis alone is not a suitable way to generate hydrogen.

Inspired by the good results of Al–$NaBH_4$ dual solid system [7,19], we present in this work a new hydrogen generation system based on an Mg–$LiBH_4$–$NiCl_2$ mixture elaborated by ball milling after a series of exploratory trials. Compared with single Mg or $LiBH_4$ system, the newly developed system has significantly optimized its hydrogen generation rate and fuel conversion. Some preliminary studies have been performed to try to understand the mechanism. And in this system, magnesium would act as the main fuel, producing hydrogen in a low cost process which is promising for portable hydrogen source applications.

2. Experimental

Mg (Sinopharm Chemical Reagent Co., Ltd, 99.0%, 100–200 mesh), $LiBH_4$ (Acros Organics, 95%), CaH_2 (Sigma Aldrich, 95%), LiH, $NiCl_2$, $NaBH_4$ (Alfa Aesar, 98%) were used as received. All sample handling was performed in an Ar filled glove box (MIKROUNA Universal) with a recirculation system. Ball milling was performed under argon atmosphere with a ball-to-powder mass ratio of 25:1 using a planetary QM-3SP4 ball miller.

The experimental setup used to measure the hydrogen generation was described in a previous paper [12]. The reaction was carried out at room temperature (298 K) and atmospheric pressure in a 250 ml flask with three openings (one for water addition, one for hydrogen exhaust, and the last one sealed with a clog). 10 ml of water was added into the flask to react with 50 mg of powder. In order to keep a constant temperature, the flask was then dipped into a water bath (298 K). The H_2 gas produced flew through a spiral condenser and entered into a glass tube containing drierite to remove water vapor. Then the gas was measured with a flow meter (ADM 2000, Agilent Technologies) which was connected to a computer to record the hydrogen generation rate (HG rate) and volume as a function of time. The background flow that was measured under the same conditions solid samples was subtracted from the original data and the values obtained were finally converted to those under the standard conditions (273 K, 1 atm) using the ideal gas equation. Each test was repeated at least twice to confirm its reproducibility (±5%). The hydrogen production yield (%) was defined as the volume of generated hydrogen over the theoretical value, which is the volume of hydrogen generated assuming all the hydrogen was completely released. The maximum hydrogen generation rate (mHGR) is defined as the largest volume of hydrogen generated *per* minute *per* gram composite. The hydrogen generation curves within the first hour were presented and discussed in this work.

X-ray diffraction (XRD) measurements were carried out by an X'Pert PRO diffractometer with Cu Kα radiation. The specific surface area of the powder was measured by N_2 adsorption (multipoint BET) using an ASIC-2 analyzer. The samples were degassed for 12 h at 250 °C to remove any moisture or adsorbed contaminants. The microstructure of the samples was observed by a scanning electron microscopy (SEM) system (SIRON), which was equipped with INCA energy dispersive X-ray spectroscopy measurements. X-ray photoelectron spectroscopy (XPS) analysis was performed on a VG ESCALAB MARK II system with Mg Kα radiation (1253.6 eV) under a base pressure of 1×10^{-8} Torr. The spectra were recorded after Ar^+ sputtering of the surface for 15 min. All the binding energies were calibrated using the C1s peak at 284.6 eV of the adventitious carbon as an internal standard.

3. Results and discussion

3.1. Effect of different hydrides addition

As the hydrolysis dependence of Mg–H_2O system on different hydrides has not been reported yet, we first examine the hydrolysis properties of Mg powder milled with 9 wt.% $LiBH_4$, $NaBH_4$, CaH_2 and LiH for 3 h. As seen in Fig. 1, compared with pure magnesium, the addition of hydrides apparently raises both the mHGR and yield. This may be due to the brittleness property of these hydrides which serve as a cutter during the milling process, reduce the grain size of Mg particles and increase its reactivity. But the reaction enters an induction period after the initial rapid reaction occurring during the first few minutes because the surface of magnesium grains was covered by the dense byproduct generated. It can be seen that the sample with $LiBH_4$ addition shows the highest yield and mHGR, about 18% and 309.4 ml min^{-1} g^{-1}, respectively. CaH_2 also possesses good activation capability showing a high mHGR of about 261.4 ml min^{-1} g^{-1}. Tessier et al. [20] formerly reported that a synergistic effect existed between MgH_2 and CaH_2, and CaH_2

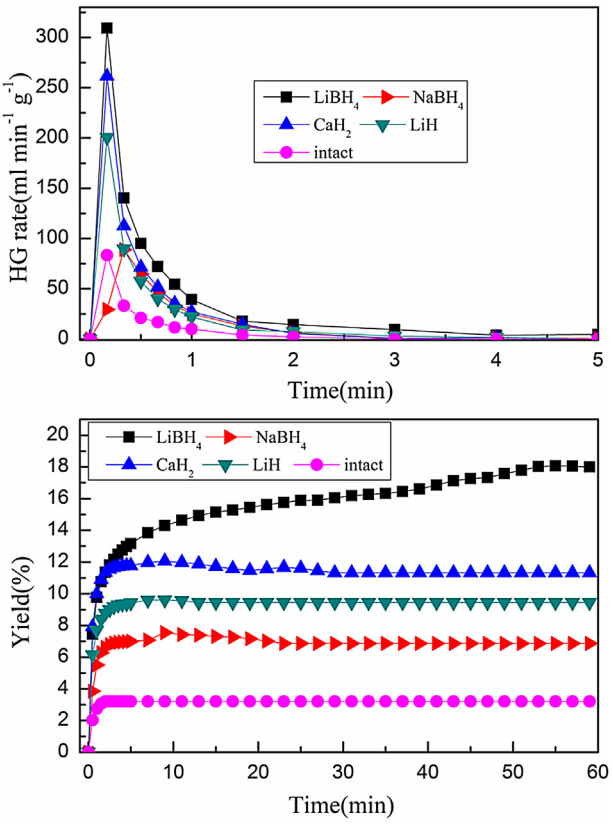

Fig. 1. HG rate (top) and yield (bottom) of Mg ball milled with 9 wt.% different hydrides for 3 h.

helped to open up the structure of MgH_2 which generated more fresh surface to react with H_2O. Presumably, this also works on this Mg-hydride system where $LiBH_4$ performs the best. Among all the hydrides added, $NaBH_4$ addition shows the smallest effect on the mHGR but still improves the yield anyway.

In the Mg–H_2O system, the addition of hydrides could significantly improve the mHGR, from 83.4 of pure Mg to 309.4 ml min^{-1} g^{-1} of Mg milled with $LiBH_4$. The generation yield has also been raised a lot. Although the highest yield of Mg–$LiBH_4$ system does not exceed 20%, it is still a promising system with a large theoretical capacity of 1307.6 ml (g of composite)$^{-1}$ for Mg-9 wt.% $LiBH_4$ composite compared to only 1018.8 ml g^{-1} for pure Mg powder.

3.2. Effects of $LiBH_4$ addition

In order to get a better understanding of the Mg–$LiBH_4$–H_2O system and further improve its performance, hydrolysis performances of samples with different compositions and milling time are tested.

Table 1 shows the hydrogen production performances of Mg–$LiBH_4$ samples with different compositions milled for 3 h. Under the same milling time, the hydrogen yield decreases with increasing addition amount of $LiBH_4$. The Mg-3 wt.% $LiBH_4$ sample reaches a yield of 22.5%, corresponding to about 250 ml H_2 (g of composite)$^{-1}$, and the numbers drop to 18% (235.4 ml g^{-1}) when the addition amount increases to 9 wt.%. Though the yield is lower, the samples with addition amounts of 27 wt.% and 36 wt.% still have a hydrogen volume (238 and 236.8 ml g^{-1}, respectively) similar to that of Mg-9 wt.% $LiBH_4$ composite since they themselves have high theoretical values. Besides, the Mg-36 wt.% composite has the highest mHGR of 475 ml min^{-1} g^{-1}. Presumably, $LiBH_4$ is more reactive and easier to hydrolyze than Mg thus catalyzing the Mg–H_2O reaction to some extent. But the rapidly formed foaming byproduct covers the surface of reactive materials and blocks the reaction. For samples with more $LiBH_4$ addition, more hydrogen will be released in the first minute and $LiBH_4$ becomes a deciding factor of mHGR. However, as the byproduct quickly accumulates, there will be less chances for Mg to react with H_2O directly if more $LiBH_4$ is added. And the overall yield is therefore lower. We also find that the samples become dangerously reactive and easily burns when the addition amount of $LiBH_4$ exceeds 18 wt.%, so these samples will not be discussed. Besides, more $LiBH_4$ added means more cost which runs contrary to the aim of this work.

Table 2 shows the hydrogen generation performances of Mg-3 wt. % $LiBH_4$ milled for different hours. It can be seen that milling time apparently exerts a significant effect on the hydrolysis properties of this Mg–$LiBH_4$ system. The hydrogen yield increases as the milling time increases. There are no significant differences within an hour and the hydrogen yield is around 12.2%. When the milling time is increased to 10 h, the yield in 60 min reaches 45.4%, corresponding to about 510 ml (g of composite)$^{-1}$. But the mHGR is 342.1 ml min^{-1} g^{-1} which is not as high as the 3 h (414.4 ml min^{-1} g^{-1}) and 6 h (418.4 ml min^{-1} g^{-1}) milled samples. This could be ascribed to the partial oxidation and cold-welding effect existing between Mg particles during the long-time milling [12], which reduces the available reactive surface area and slows down the reaction rate in the first few minutes.

As seen in Fig. 2 which shows SEM images of Mg (a), sample 3 (b) and 4 (c), respectively. By milling with $LiBH_4$ the shapes of Mg grains (a) are changed from initial compact bulk material to platelet with fractured surface. The BET measurements have been performed to confirm its change in particle size. The results show that the specific surface area of pure Mg powder is hardly detectable (approx. 0.04 m^2 g^{-1}). And sample 3 has an area of 0.27 m^2 g^{-1}, while the area of sample 4 is 0.43 m^2 g^{-1}. The decrease of grain size as well as the severe plastic deformation and defects induced in the milling process, such as dislocations [21], combines to promote the hydrolysis reaction. In short, the hydrolysis properties of this Mg–$LiBH_4$ system can be improved by changing the milling conditions, but the results are not satisfactory (the highest yield being only 22.5%). Some other means should be taken to further optimize its yield and mHGR.

Table 1
Hydrogen generation performances of Mg-*x* wt. %$LiBH_4$ ball milled for 3 h (x = 3, 9, 18, 27, 36).

Sample #	Amount of $LiBH_4$ (wt.%)	Milling time (h)	Hydrogen generation within 60 min (ml g^{-1})	Yield (%)	Maximum hydrogen generation rate (ml min^{-1} g^{-1})
1	3	3	250.0	22.5	414.4
2	9	3	235.4	18.0	376.3
3	18	3	189.6	12.2	388.3
4	27	3	238.0	13.5	425.0
5	36	3	236.8	12.2	475.0

Table 2
Hydrogen generation performances of Mg-3 wt.% $LiBH_4$ milled for different hours.

Sample #	Amount of $LiBH_4$ (wt.%)	Milling time (h)	Hydrogen generation within 60 min (ml g^{-1})	Yield (%)	Maximum hydrogen generation rate (ml min^{-1} g^{-1})
1	3	0.5	146.0	13.0	362.7
2	3	1.0	115.5	10.3	322.1
3	3	3.0	250.0	22.5	414.4
4	3	6.0	321.0	28.6	418.1
5	3	10.0	510.0	45.4	342.1

3.3. Effects of $NiCl_2$ addition

As mentioned above, by milling with salts [13], such as $MgCl_2$, the hydrolysis performance of Mg powder has been greatly improved. Although has not been studied before, the positive effect of $NiCl_2$ on the hydrolysis properties of magnesium can be expected. As a kind of catalyst, $NiCl_2$ has already been confirmed to benefit the destabilisation of $LiBH_4$ for hydrogen storage materials [22,23]. And the addition of $NiCl_2$ might also affect the hydrolysis properties of $LiBH_4$ to promote the overall yield as well.

In order to study the effects of $NiCl_2$ on the hydrolysis of Mg–$LiBH_4$, we conduct sets of experiments with $NiCl_2$ addition and compare the results with those of samples without $NiCl_2$ listed above in Table 1. As can be seen in the top of Fig. 3, hydrogen generation is greatly improved by adding $NiCl_2$ to the original composite. The yield of 3 h milled Mg-3 wt.% $LiBH_4$ samples is raised from 22.5% to 59.5%. Similarly, the Mg-9 wt. %$LiBH_4$ (18%–65.8%) and Mg-18 wt.% $LiBH_4$ (12%–83.4%) samples also show better performances. It is evident that the most impressive improvement comes from the Mg-18 wt.% $LiBH_4$ composite with the yield increased by nearly seven-fold and mHGR (1400 ml min^{-1} g^{-1}) by nearly four-fold. The 9 wt. % $LiBH_4$ added sample possesses the highest mHGR of 1655 ml min^{-1} g^{-1}. It can be concluded that with the same addition amount of $NiCl_2$, the 18 wt. % addition of $LiBH_4$ seems to be appropriate for a hydrogen source for its high yield and theoretical hydrogen capacity.

The addition of $NiCl_2$ into Mg–$LiBH_4$ system proves successful and there is still room for optimization. The milling time and

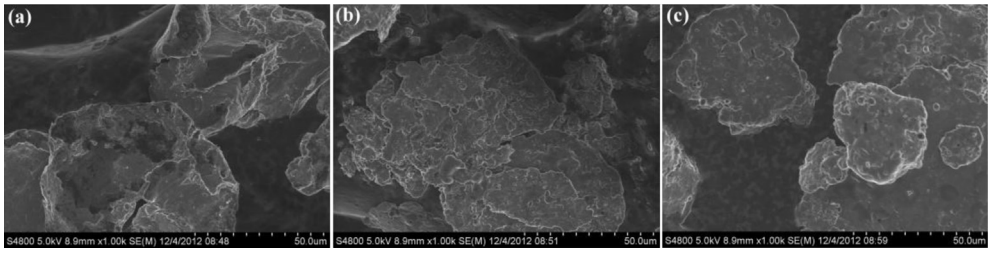

Fig. 2. SEM images of Mg powder (a), Mg-3 wt. %$LiBH_4$ ball-milled for 3 h (b) and 6 h (c).

composition are changed to examine the hydrolysis properties of this Mg–$LiBH_4$–$NiCl_2$ system. Table 3 shows the hydrogen generation performances of Mg-18 wt.% $LiBH_4$-10 wt.% $NiCl_2$ milled for different hours. It can be seen that the hydrogen yield increases when the milling time is prolonged. The 3 h milled sample shows good hydrolysis ability as formerly stated. But the yield of the 6 h milled sample is even higher, reaching 91.7%. One reason might be that $LiBH_4$ and $NiCl_2$ serving as cutter prevent the cold-welding of Mg powder, reduce its grain size and increase its reactive surface area as can be seen in the SEM pictures. Fig. 4 shows the SEM images of Mg-18 wt.% $LiBH_4$-10 wt.% $NiCl_2$ samples with milling time ranging from 0.5 h to 6 h. It is clear that the grain size decreases when the milling time is increased. Similar to Mg powder, the specific surface area of 0.5 h milled sample is also very mall (approx. 0.08 $m^2\ g^{-1}$). The area of 3 h milled sample is 1.21 $m^2\ g^{-1}$, which is smaller than 2.09 $m^2\ g^{-1}$ of the 6 h milled sample. Note that the grain size of Mg–$LiBH_4$–$NiCl_2$ composites is even smaller than those of the samples with only $LiBH_4$ addition as shown in Fig. 2. Fig. 5 shows the EDS mapping of Mg-18.

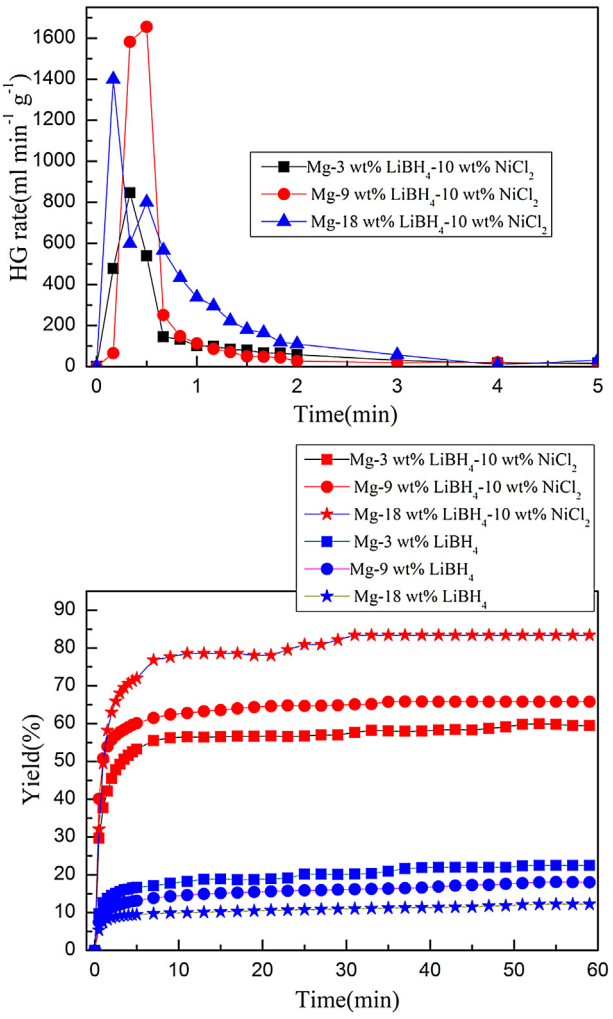

Fig. 3. Hydrogen yield (top) and HG rate (bottom) of Mg–$LiBH_4$ composites with $NiCl_2$ addition ball milled for 3 h in comparison of the same Mg–$LiBH_4$ composites without $NiCl_2$ addition (listed in Table 1).

Fig. 5 shows the hydrogen generation and mHGR curves of Mg-18 wt. % $LiBH_4$ with different addition amounts of $NiCl_2$ milled for 6 h. The yield is higher if more $NiCl_2$ is added, increasing from 51.3% of 1 wt. % addition to 96.1% of 15 wt. % addition. As for the mHGR, the tendency is similar, and the values increase from 324 ml $min^{-1}\ g^{-1}$–1113.3 ml $min^{-1}\ g^{-1}$. It can be seen that $NiCl_2$ is an useful activator that generates positive effects on Mg powder or even $LiBH_4$. As a salt, $NiCl_2$ hinders the agglomeration of Mg powder to decrease the grain size during the ball milling (seen in Fig. 4) and promotes the corrosion in the hydrolysis process which will be discussed below. The EDS mapping shown in Fig. 6 also confirms that $NiCl_2$ has been uniformly dispersed into the Mg–$LiBH_4$ mixture after the milling process. As a catalyzer usually used in hydrogen storage materials [3,22,23], $NiCl_2$ may also have some effect on catalyzing the hydrolysis of $LiBH_4$, which needs to be verified in the future works. In a word, the hydrolysis properties of Mg–$LiBH_4$ system have been greatly improved by $NiCl_2$ addition.

Fig. 7 shows the XRD analysis results of Mg-18 wt. %$LiBH_4$-15 wt. %$NiCl_2$ composites after milling and hydrolysis, respectively. The peaks of Mg can be easily recognized in the XRD patterns obtained after milling. Some peaks that belong to $LiBH_4$, $MgCl_2$ and $NiCl_2$ also appear. $MgCl_2$ is a new compound generated during the milling process, which indicates that the redox reaction between Mg and $NiCl_2$ might be triggered during the ball-milling:

$$Mg + NiCl_2 \rightarrow MgCl_2 + Ni \quad (1)$$

In the patterns obtained after hydrolysis, peaks belonging to $LiBH_4$ disappear but some broadened peaks of residual Mg are found. The relative intensity of these peaks has been remarkably decreased which proves that the hydrolysis reaction has been carried out almost completely. Peaks of byproduct $Mg(OH)_2$ can also

Table 3
Hydrogen generation performances of Mg-18 wt. % $LiBH_4$-10 wt. % $NiCl_2$ ball milled for different hours.

Sample #	Milling time (h)	Hydrogen generation within 60 min (ml g^{-1})	Yield (%)	Maximum hydrogen generation rate (ml $min^{-1}\ g^{-1}$)
1	0.5	498.5	34.9	370.5
2	1.0	633.0	46.4	876.2
3	3.0	1137.8	83.4	1400.0
4	6.0	1251.0	91.7	910.0

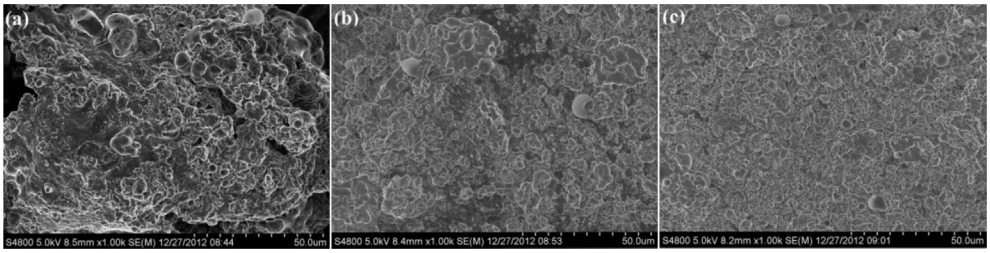

Fig. 4. SEM images of the Mg-18 wt. %$LiBH_4$-10 wt. %$NiCl_2$ ball milled for 0.5 h (a), 3 h (b) and 6 h (c).

be recognized but their intensity is much weaker than expected. This is probably due to the fact that the byproduct exists as amorphous state or nanocrystalline after hydrolysis which could be supported by the apparent broadening and weakening of the peaks shown in the pattern.

3.4. Mechanistic study

Many studies [24,25] have suggested that the overall Mg–H_2O reaction should follow Eq. (2), and the hydrolysis of $LiBH_4$ [8] has been expressed as Eq. (3).

$$Mg + 2H_2O \rightarrow H_2 + Mg(OH)_2 \quad (2)$$

$$LiBH_4 + 2H_2O \rightarrow LiBO_2 + 4H_2 \quad (3)$$

As ball-milling is widely used as a method to activate materials [12,20,26,27], $LiBH_4$ here is used as an additive and milled with Mg powder. With its brittleness property, $LiBH_4$ serves as a cutter and opens up the structure of Mg grains during ball milling. The grain size of Mg powder is thereby decreased which enlarges the specific area and optimizes its reactivity. Besides, many defects generated inside the grain will also facilitate the corrosion of Mg, and $LiBH_4$ itself is also activated at the same time. As hydrides are easier to hydrolyze than Mg, the activated $LiBH_4$ quickly reacts with water to initiate the overall reaction. Meanwhile, the large heat released can also accelerate the kinetics locally.

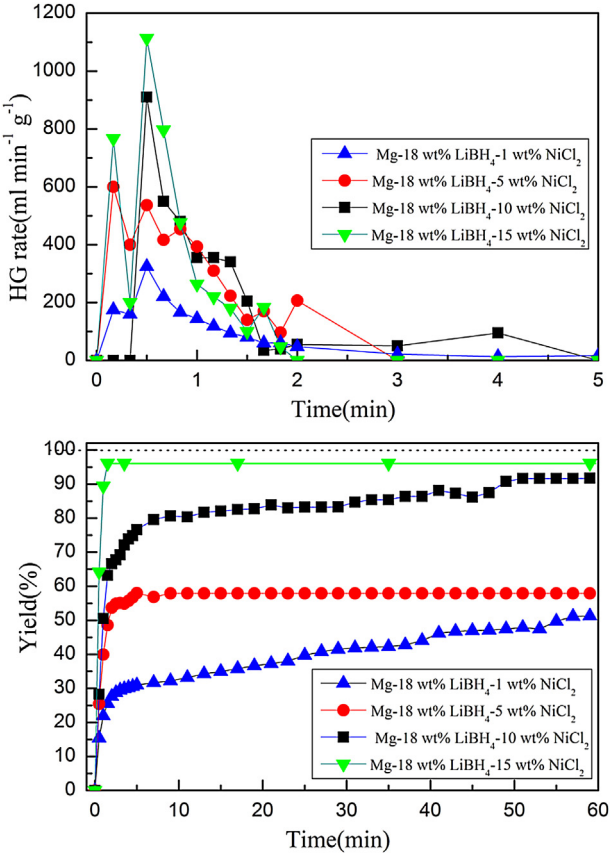

Fig. 5. HG rate (top) and hydrogen yield (bottom) of Mg-18 wt. % $LiBH_4$ with different addition amount of $NiCl_2$ milled for 6 h.

Similarly, the addition of $NiCl_2$ also contributes to the decrease of the grain size and is most likely to be the main factor, which can be concluded from Figs. 2 and 4. Besides, salt particles are driven into newly created surfaces of Mg grains, produce salt gates [28] that will be removed in water environment and form a pass way for water to enter and react with freshly exposed surface of Mg. The Cl^- generated through the salt dissolution is believed to be associated with the destabilization of the $Mg(OH)_2$ passive layer [25,29]. The Cl^- ions substitute OH^- ions to form $MgCl_2$ which leads to localized breakdown of the passive layer by a pitting process. It is claimed [29] that the existence of Cl^- might also accelerate the electrochemical reaction rate from magnesium to magnesium univalent ions. The electrolyte solution formed by the hydrolysis of $LiBH_4$ and $NiCl_2$ can also enhance the micro galvanic effect that will be discussed below.

What's more, the XRD patterns shown in Fig. 7 indicate that metallic Ni might be generated through Eq. (1). But the addition of $LiBH_4$ makes it possible to be generated by another way. Graetz et al. [30] found that Ni^{2+} was reduced to primarily Ni^0 and formed a disordered nanocluster Ni_3B after ball milling with $LiBH_4$ by the following equation [3]:

$$6LiBH_4 + 3NiCl_2 \rightarrow 6LiCl + Ni_3B + 5B + 12H_2 \quad (4)$$

However, the addition amount of both $NiCl_2$ and $LiBH_4$ is apparently much smaller than the main material Mg and this reaction might not be carried out completely. As a result, metallic Ni mainly comes from Eq. (1). In order to confirm its existence, an XPS analysis is performed on the Mg-18 wt.% $LiBH_4$-15 wt.% $NiCl_2$ ball milled for 6 h sample, as shown in Fig. 8. Peaks of metallic Mg (BE, 49.7 eV) [31] can be identified. And peaks at 853.6 eV and 857.4 eV can be assigned to metallic Ni and $NiCl_2$ [32]. Peak belonging to $MgCl_2$ (BE, 51.6 eV) is not obvious because its signal is covered by that of the bulk metallic Mg.

The metallic Ni particles generated during ball-milling deposit on the surface of Mg to form numerous micro galvanic cells, wherein Ni particles act as cathode centers during water splitting. And magnesium is well known for its high susceptibility to these galvanic attacks [29]. So Ni, with a low hydrogen overpotential, could induce sever corrosion of Mg by forming those galvanic cells, promoting the hydrolysis kinetics and yield. What's more, the addition of $NiCl_2$ also brings about another important effect contributing to the high mHGR and yield obtained. We believe that the locally inhibition of the repassivation of Mg caused by the

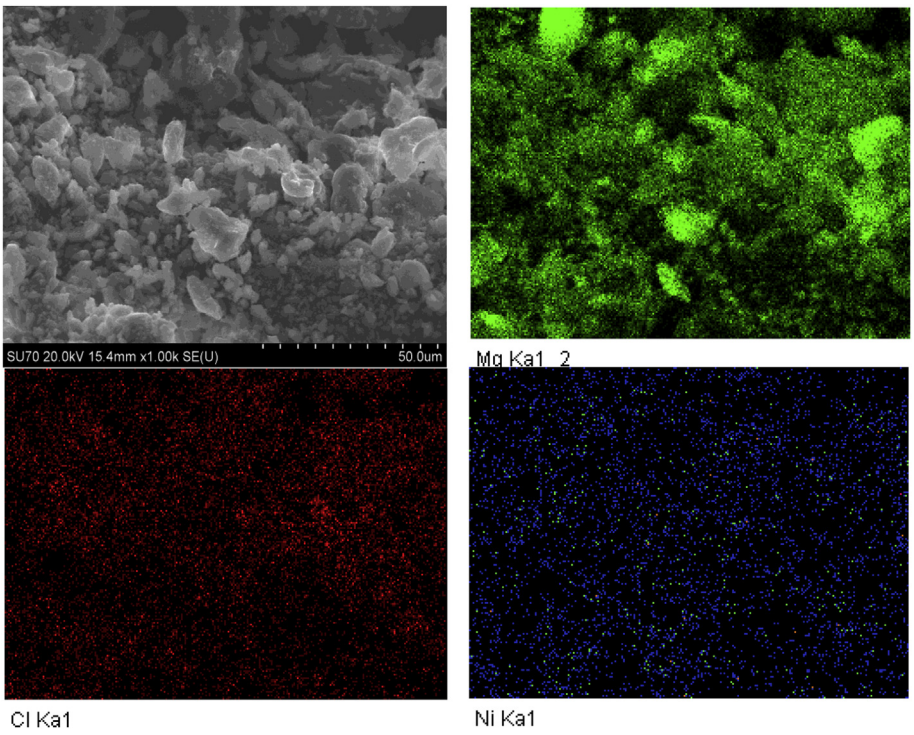

Fig. 6. EDS mapping of Mg-18 wt.% $LiBH_4$-15 wt.% $NiCl_2$ ball milled for 6 h.

formation of metallic Ni is also a vital factor leading to the great improvement of the hydrolysis of this Mg–$LiBH_4$–$NiCl_2$ system. The freshly generated Ni particles deposit on the surface of magnesium and keep the activated Mg powder from being repassivated by oxides before the electrochemical corrosion could have occurred. This may also account for the relationship between hydrogen yield and $NiCl_2$ content shown in Fig. 5. But more work needs to be done to further understand the mechanism of the inhibition process caused by the metallic Ni as well as the catalytic effect between $LiBH_4$ and $NiCl_2$.

4. Conclusions

A new method of promoting the hydrolysis properties of Mg–H_2O system has been established by ball milling Mg with $LiBH_4$ and $NiCl_2$. $LiBH_4$ alone could improve the reaction kinetics and yield to some extent but is still not satisfactory. And with the addition of $NiCl_2$ the overall hydrogen generation performances have been greatly optimized. The Mg-18 wt. %$LiBH_4$-15 wt. %$NiCl_2$ sample ball-milled for 6 h reaches a yield of 96.1% with an mHGR of 1113.3 ml min^{-1} g^{-1}. Preliminary mechanics studies show that through ball milling process, the grain size of Mg powder is decreased. And the fast hydrolysis of hydride and dissolution of salt initiate the overall reaction, provide vacancies for water penetration and induce pit corrosion. Besides, the heat released boosts the kinetics locally. In particular, the metallic Ni formed during the milling process deposits on the surface of Mg and most likely acts as local inhibitors to the repassivation of Mg. In a word, the newly found Mg–$LiBH_4$–$NiCl_2$ hydrolysis system proved to be a promising

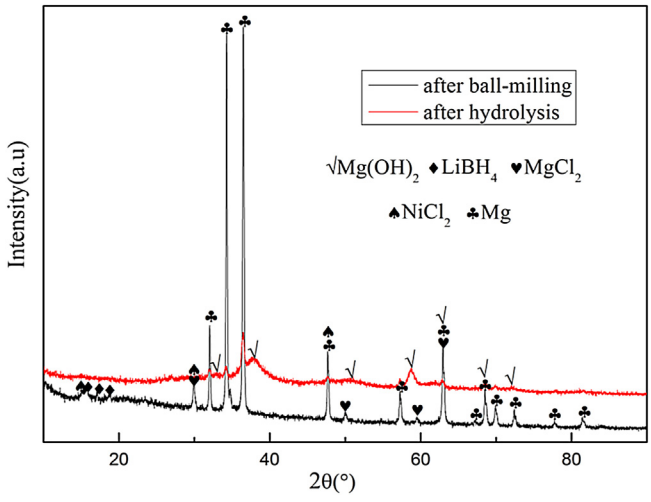

Fig. 7. X-ray patterns of Mg-18 wt. %$LiBH_4$-15 wt. %$NiCl_2$ samples after ball milling and hydrolysis.

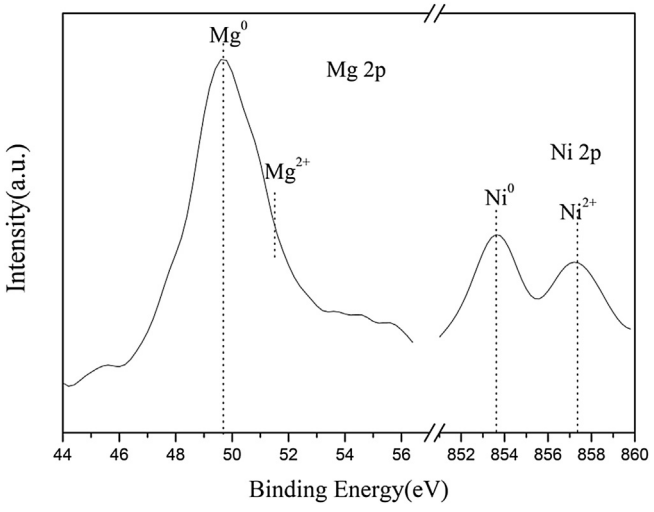

Fig. 8. XPS spectra of Mg 2p, Ni 2p levels for the sample Mg-18 wt.% $LiBH_4$-15 wt.% $NiCl_2$ ball milled for 6 h.

method to produce hydrogen for mobile or portable applications, which further contributes to the development of on-board hydrogen fuel cells.

Acknowledgments

This work was supported by the National Basic Research Program of China (973 Program) (no. 2010CB631304), National Natural Science Foundation of China (no. 51171168), Zhejiang Provincial Natural Science Foundation of China (no. Y4110147), Key Science and Technology Innovation Team of Zhejiang Province (no. 2010R50013).

References

[1] Z.Y. Deng, W.H. Liu, W.Z. Gai, Y. Sakka, J.H. Ye, Z.W. Ou, J. Am. Ceram. Soc. 93 (2010) 2534–2536.
[2] L. Schlapbach, A. Zuttel, Nature 414 (2001) 353–358.
[3] J. Shao, X. Xiao, L. Chen, X. Fan, S. Li, H. Ge, Q. Wang, J. Mater. Chem. 22 (2012) 20764–20772.
[4] L. Soler, J. Macanás, M. Muñoz, J. Casado, J. Power Sources 169 (2007) 144–149.
[5] M.-Q. Fan, L.-X. Sun, F. Xu, Energy 35 (2010) 1333–1337.
[6] S.C. Amendola, S.L. Sharp-Goldman, M.S. Janjua, M.T. Kelly, P.J. Petillo, M. Binder, J. Power Sources 85 (2000) 186–189.
[7] M.-Q. Fan, S. Liu, W.-Q. Sun, Y. Fei, H. Pan, C.-J. Lv, D. Chen, K.-Y. Shu, Int. J. Hydrogen Energy 36 (2011) 15673–15680.
[8] U.B. Demirci, O. Akdim, P. Miele, J. Power Sources 192 (2009) 310–315.
[9] U.B. Demirci, O. Akdim, P. Miele, Int. J. Hydrogen Energy 34 (2009) 2638–2645.
[10] J.-Y. Uan, C.-Y. Cho, K.-T. Liu, Int. J. Hydrogen Energy 32 (2007) 2337–2343.
[11] S.-H. Yu, J.-Y. Uan, T.-L. Hsu, Int. J. Hydrogen Energy 37 (2012) 3033–3040.
[12] M.H. Grosjean, M. Zidoune, L. Roue, J.Y. Huot, Int. J. Hydrogen Energy 31 (2006) 109–119.
[13] M.H. Grosjean, L. Roue, J. Alloys Compd. 416 (2006) 296–302.
[14] K. Chlopek, C. Frommen, A. Leon, O. Zabara, M. Fichtner, J. Mater. Chem. 17 (2007) 3496–3503.
[15] L. Li, F. Qiu, Y. Wang, Y. Wang, G. Liu, C. Yan, C. An, Y. Xu, D. Song, L. Jiao, H. Yuan, J. Mater. Chem. 22 (2012) 3127–3132.
[16] V.C.Y. Kong, F.R. Foulkes, D.W. Kirk, J.T. Hinatsu, Int. J. Hydrogen Energy 24 (1999) 665–675.
[17] Y. Kojima, Y. Kawai, M. Kimbara, H. Nakanishi, S. Matsumoto, Int. J. Hydrogen Energy 29 (2004) 1213–1217.
[18] B. Weng, Z. Wu, Z. Li, H. Yang, H. Leng, J. Power Sources 196 (2011) 5095–5101.
[19] L. Soler, J. Macanas, M. Munoz, J. Casado, Int. J. Hydrogen Energy 32 (2007) 4702–4710.
[20] J.P. Tessier, P. Palau, J. Huot, R. Schulz, D. Guay, J. Alloys Compd. 376 (2004) 180–185.
[21] N.V. Kazantseva, N.V. Mushnikov, A.G. Popov, P.B. Terent'ev, V.P. Pilyugin, J. Alloys Compd. 509 (2011) 9307–9311.
[22] F.E. Pinkerton, M.S. Meyer, G.P. Meisner, M.P. Balogh, J. Alloys Compd. 433 (2007) 282–291.
[23] B.J. Zhang, B.H. Liu, Int. J. Hydrogen Energy 35 (2010) 7288–7294.
[24] C.Y. Cho, K.H. Wang, J.Y. Uan, Mater. Trans. 46 (2005) 2704–2708.
[25] G.L. Makar, J. Kruger, J. Electrochem. Soc. 137 (1990) 414–421.
[26] M.H. Grosjean, M. Zidoune, J.Y. Huot, L. Roue, Int. J. Hydrogen Energy 31 (2006) 1159–1163.
[27] P. Dupiano, D. Stamatis, E.L. Dreizin, Int. J. Hydrogen Energy 36 (2011) 4781–4791.
[28] B. Alinejad, K. Mahmoodi, Int. J. Hydrogen Energy 34 (2009) 7934–7938.
[29] G.L. Song, A. Atrens, Adv. Eng. Mater. 1 (1999) 11–33.
[30] J. Graetz, S. Chaudhuri, T.T. Salguero, J.J. Vajo, M.S. Meyer, F.E. Pinkerton, Nanotechnology 20 (2009) 204007.
[31] W.S.J. Moulder, P. Sobol, K. Bomben, in: J. Chastain (Ed.), Handbook of X-ray Photoelectron Spectroscopy, Perkin–Elmer, Eden Prairie, MN, 1992.
[32] R.B. Diegle, N.R. Sorensen, C.R. Clayton, M.A. Helfand, Y.C. Yu, J. Electrochem. Soc. 135 (1988) 1085–1092.